Impact Control in Hydraulic Actuators with Friction: Theory and Experiments

P. Sekhavat, **Q.Wu** and **N. Sepehri***

Department of Mechanical and Industrial Engineering
The University of Manitoba
Winnipeg, Manitoba, Canada R3T 5V6

Abstract- Stabilizing manipulators during the transition from free motion to constraint motion is an important issue in contact task control design. In this paper, a Lyapunov-based control scheme is introduced to regulate the impact of a hydraulic actuator coming in contact with a nonmoving environment. Due to the discontinuous nature of friction model and the proposed control law, existence, continuation and uniqueness of Filippov's solution to the system are first proven. Next, the extension of LaSalle's invariance principle to nonsmooth systems is employed to prove that all the solution trajectories converge to the equilibria. The controller is tested experimentally to verify its practicality and effectiveness in collisions with hard and soft environments and with various approach velocities.

1 Introduction

One issue in robotic applications is a proper interaction between the manipulator and the environment. The manipulator should be able to follow a free space trajectory and make a stable contact with the environment while the energy of impacts is dissipated and the desired contact force is achieved. Such tasks can be divided into three modes of motion: free-motion, constraint-motion, and the transition mode between the two. Despite the existence of various control schemes for contact task problem, only a few recent studies have dealt with the transition mode as a separate mode of motion with special treatment.

Pagilla and Yu [1] proposed separate control laws for free trajectory tracking, constrained motion and transition phase between the two and experimentally studied the performances of the system in slow/fast collisions. Xu et al. [2] incorporated joint acceleration and velocity feedbacks into an integral force control to suppress the impact bouncings. Tarn et al. [3] used acceleration feedback to control the transient force response and to reduce the impulsive force and bouncings.

Contact task control of hydraulically actuated systems has not yet received enough attention, much less the control in the transient phase. This is mainly due to the highly nonlinear characteristics of the hydraulic systems. Also, employing a proper impact model that incorporates the realistic bouncing, local elastic deformations and energy dissipations in the analysis contributes to the challenges of the problem. Actuator friction due to piston-cylinder sealing is another problem in hydraulic manipulations degrading the system performance and making precise control difficult to achieve. These non-idealities necessitate nonlinear control design for impact control of hydraulic actuators.

In the present study, a Lyapunov-based transition control algorithm is introduced that could effectively regulate the possible impacts of a hydraulic actuator during the transition phase from free to constrained motion. Upon sensing a nonzero force, the controller positions the actuator at the location where the onset of the force was sensed. Measurements of the ram position, hydraulic line pressures, supply pressure and the knowledge about the direction of the valve spool displacement are the only requirements of the control scheme. The controller does not require continuous force or velocity feedback as they are difficult to measure throughout the short transition phase. Although no knowledge of the impact dynamics, friction effects, servovalve dynamics, or hydraulic parameters is required for control action, stability and effectiveness of the control scheme considering all above factors is verified both analytically and experimentally. Particularly, solution and stability analyses of the system are conducted using the Hertz-type contact model that incorporates the realistic bouncings, local elastic deformations and energy dissipations in the analyses.

Due to the discontinuous nature of the actuator friction model and the proposed control law, the system is nonsmooth. Here, existence, continuation and uniqueness of the solution to the system are studied using Filippov solution theories [4]. The extension of Lyapunov stability theory to nonsmooth systems [5] is then employed to guarantee the global asymptotic convergence of the systems trajectories to equilibria. It is shown that the position steady state error remains bounded in a small range adjustable by selecting proper controller gains based on Lyapunov direct method. For actuators with negligible friction, the system is guaranteed to be asymptotically stable about its unique equilibrium point located on the surface of the environment. The controller is tested experimentally to verify its

This work was supported by the Natural Sciences and Engineering Research Council of Canada (NSERC) and the Institute for Robotics and Intelligent Systems (IRIS) Network Centre of Excellence.

* Corresponding author: nariman@cc.umanitoba.ca

practicality and effectiveness in collisions with different environments and with various approach velocities.

2 Dynamic Model of the System

The system under study is composed of a hydraulic actuator coming in contact with a non-moving environment (Fig. 1). The equation of motion of the system is:

$$m\ddot{x} = AP_L - F_f - F_{imp} \tag{1}$$

where x is the piston displacement, F_f is the friction force, and F_{imp} is the impact force. Parameters m and A are the mass of actuator's moving parts and piston area, respectively. P_L=P_i-P_o is the load pressure. For valves with rectangular matched and symmetric orifice areas, P_L changes with time according to the following relation (neglecting leakages) [6]:

$$\dot{P}_L = \frac{1}{C}\left(-A\dot{x} + \frac{c_d w}{\sqrt{\rho}} x_{sp}\sqrt{P_s - sign(x_{xp})P_L} \right) \tag{2}$$

where $\dot{x}$ is the actuator velocity, w is the orifice area gradient, c_d is the orifice coefficient of discharge, ρ is the hydraulic fluid density, P_s is the pump pressure, and x_{sp} is the spool displacement. $C = V_t/4\beta$ is the hydraulic compliance where V_t is the total actuator volume and β is the effective bulk modulus of the system.

The function $sign(x_{sp})$ in (2) is defined as:

$$sign(x_{sp}) = \begin{cases} x_{sp}/|x_{sp}| & ; \quad x_{sp} \neq 0 \\ 0 & ; \quad x_{sp} = 0 \end{cases} \tag{3}$$

The dynamics between the spool displacement, x_{sp}, and input voltage, u, is modeled as a first-order system which is valid for applications operating at low frequencies [7]:

$$\dot{x}_{sp} = -\frac{1}{\tau}x_{sp} + \frac{k_{sp}}{\tau}u \tag{4}$$

k_{sp} and τ are valve gain and time constant, respectively.

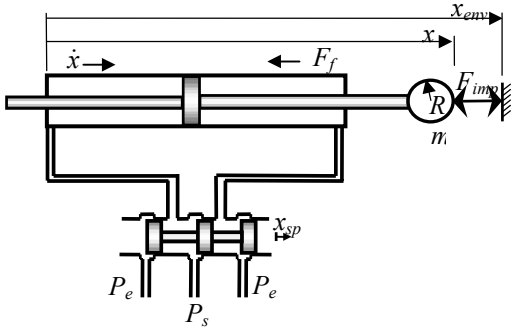

Fig. 1 Schematic of hydraulic actuator-environment

The Hertz-type contact model is employed to represent the real behavior of the system during impact [8]. The model has been used by many researchers and incorporates the realistic bouncings, local elastic deformations and energy dissipations in the analysis:

$$F_{imp} = \begin{cases} (1+p\dot{x})H(x-x_{env})^n & (x-x_{env}>0)\,\&\,(1+p\dot{x}>0) \\ 0 & otherwise \end{cases} \tag{5}$$

In (5), x_{env} is the position of the environment. n and H are constants that depend on material and geometric properties of the colliding bodies. p denotes energy loss (damping) parameter during collision. Its value is related to the coefficient of restitution and approach velocity.

Various experimental works have confirmed the Tustin's discontinuous friction model as a valid representation of friction in many applications and hydraulic systems [9]:

$$F_f = \left[F_C + (F_S - F_C)e^{-(\dot{x}/\dot{x}_s)^2}\right]\mathrm{sgn}(\dot{x}) + d\,\dot{x} \tag{6}$$

F_C is the Coulomb friction, F_S is the stiction force (breakaway force), $\dot{x}_s$ is a threshold velocity where the downward bend in friction appears after the stiction force is surmounted, and d is the viscous friction coefficient. At rest, the friction (F_S sgn(0)) is opposite to the net external force and can acquire any value in the range of $[-F_S, F_S]$. This opposing static friction increases with the increase in the net external force until it reaches the breakaway force, F_S, where the piston starts to slide and the friction drops due to Stribeck effect. The function $\mathrm{sgn}(\dot{x})$ is, thus, defined as:

$$\begin{cases} \mathrm{sgn}(\dot{x}) = \{\dot{x}/|\dot{x}|\} & : \quad \dot{x} \neq 0 \\ \mathrm{sgn}(\dot{x}) \in [-1,1] & : \quad \dot{x} = 0 \end{cases} \tag{7}$$

3 Controller Design

The goal of this section is to design a controller that rests the hydraulic actuator on the surface of an unknown colliding environment. Sensing the first nonzero force denotes the impact occurrence and the environment location, x_{env}, is recorded as the position of the implement at that time.

The control scheme is designed based on the Lyapunov direct method (detailed in Section 5):

$$u = -\frac{K_p P_S P_L + K_x(x - x_{des})(P_s - sign(x_{sp})\,P_L)}{\sqrt{P_s - sign(x_{sp})\,P_L}} \tag{8}$$

K_p and K_x are positive constant gains and $sign(e_4)$ is as defined in (3). The proposed control law has the following unique features:

i) It does not require measurement of the interaction force (F_{imp}) feedback as it is not realistic to assume that the interaction force is measurable and can be compensated for, during short transition phase.

ii) No velocity feedback in the control law prevents practical drawbacks in high stiffness collisions.

iii) Measurements of the ram position, hydraulic line pressures, supply pressure and the knowledge about the direction of the valve spool displacement are the only requirements of the controller. No knowledge of the environmental characteristics, friction nature, or hydraulic parameters is required for the control action.

Note that in practice, $(P_s - sign(x_{sp})P_L)$ is seldom zero since $|P_L|$ is seldom close to P_s. In the rare cases that it becomes zero (e.g., due to any noise), it will be set to a

small positive number to avoid the problem of large control output (a similar approach used in reference [7]).

In order to constitute the state space model of the system, the vector of error states are defined as $\mathbf{e} = (e_1, e_2, e_3, e_4)^T$:

$$e_1 = x - x_{des} \quad , \quad e_2 = \dot{x} \quad , \quad e_3 = P_L \quad , \quad e_4 = x_{sp} \tag{9}$$

Combining equations (1)-(8) yields:

$$\begin{cases} \dot{e}_1 = e_2 & \text{(10a)} \\ \dot{e}_2 = \dfrac{A}{m} e_3 - \dfrac{\left(F_C + (F_S - F_C) e^{-(e_2/\dot{x}_s)^2}\right)\text{sgn}(e_2) + d\, e_2}{m} - \dfrac{F_{imp}}{m} & \text{(10b)} \\ \dot{e}_3 = -\dfrac{A}{C} e_2 + \dfrac{c_d w}{C\sqrt{\rho}} e_4 \sqrt{P_s - sign(e_4)\, e_3} & \text{(10c)} \\ \dot{e}_4 = -\dfrac{e_4}{\tau} - \dfrac{k_{sp}\left(K_p P_s e_3 + K_x e_1 (P_s - sign(e_4)\, e_3)\right)}{\tau \sqrt{P_s - sign(e_4)\, e_3}} & \text{(10d)} \end{cases}$$

where F_{imp} in the error space is:

$$F_{imp} = \begin{cases} (1 + p\, e_2) H\, e_1^n & (e_1 > 0)\ \&\ (1 + p e_2 > 0) \\ 0 & otherwise \end{cases} \tag{11}$$

The equilibria of the above system is obtained by equating the right-hand side of (10) to zero:

$$\begin{cases} e_{2ss} = 0 \\ A e_{3ss} - F_S\, \text{sgn}(0) - \widetilde{F}_{imp} = 0 \\ e_{4ss} = 0 \\ K_p e_{3ss} + K_x e_{1ss} = 0 \end{cases} , \quad \widetilde{F}_{imp} = \begin{cases} H\, e_{1ss}^n & e_{1ss} > 0 \\ 0 & e_{1ss} \leq 0 \end{cases} \tag{12}$$

This leads to the following equilibria for the system:

$$\begin{cases} e_{1ss} = -\dfrac{K_p}{K_x} \dfrac{F_S\, \text{sgn}(0) + \widetilde{F}_{imp}}{A} \\ e_{2ss} = 0 \\ e_{3ss} = \dfrac{F_S\, \text{sgn}(0) + \widetilde{F}_{imp}}{A} \\ e_{4ss} = 0 \end{cases} \tag{13}$$

Note that $F_S\, \text{sgn}(0) \in [-F_S, F_S]$ represents the static friction at the equilibrium point. It is equal and opposite to the net external force. Therefore, the equilibrium point of the system could be every $\mathbf{e}_{eq} = (e_{1ss}, 0, e_{3ss}, 0)^T$ with

$$e_{1ss} = -\frac{K_p}{K_x} \frac{F_S\, \text{sgn}(0) + \widetilde{F}_{imp}}{A} \in \left[-\frac{K_p}{K_x} \frac{F_S + \widetilde{F}_{imp}}{A}, -\frac{K_p}{K_x} \frac{-F_S + \widetilde{F}_{imp}}{A} \right]$$

$$e_{3ss} = \frac{F_S\, \text{sgn}(0) + \widetilde{F}_{imp}}{A} \in \left[\frac{-F_S + \widetilde{F}_{imp}}{A}, \frac{F_S + \widetilde{F}_{imp}}{A} \right] \tag{14}$$

According to (14), if the actuator stops with no contact with the environment, $e_{1ss} < 0$ and $\widetilde{F}_{imp}$=0; thus, from (12), we have $e_{1ss} \in \left[-\dfrac{K_p}{K_x} \dfrac{F_S}{A}, 0 \right]$ and $e_{3ss} \in \left[0, \dfrac{F_S}{A} \right]$.

When the actuator remains at rest while in contact with the environment, we have $e_{1ss} > 0$ and $\widetilde{F}_{imp} = H\, e_{1ss}^n$. From (12), we will have

$$e_{3ss} = -\frac{K_x}{K_p} e_{1ss} \tag{15}$$

$$-\frac{K_x}{K_p} e_{1ss} - \frac{H\, e_{1ss}^n}{A} = \frac{F_S\, \text{sgn}(0)}{A} \tag{16}$$

Since the maximum value of $|F_S\, \text{sgn}(0)|$ is F_S, (16) implies that decreasing K_p / K_x would reduce the bound on maximum possible position error e_{1ss} in contact region.

The above discussion concludes that choosing a small K_p / K_x can effectively counteract frictional effects in the proposed impact control scheme and locate the actuator end-effector in a close vicinity of the surface of the environment. However, as will be seen in Section 5, restrictions on the system's Lyapunov function prevent choosing the ratio arbitrarily small. It may also be useful to note that in the absence of friction, the equilibrium point of the system would be $\mathbf{e}_{eq} = (0,0,0,0)^T$.

Due to the discontinuity of the friction model (sgn function) and the control law (*sign* function), the above control system is nonsmooth and the solution analysis should first be investigated. In the next section, Filippov's solution analysis [4] of the above system is presented.

4 Solution Analysis

According to (10), the discontinuity surface of the system is one of the following three surfaces:

$$Surface\,1 \quad S_1^3 := \{\mathbf{e} : e_2 = 0\ \&\ e_4 \neq 0\} \tag{17a}$$

$$Surface\,2 \quad S_2^3 := \{\mathbf{e} : e_2 \neq 0\ \&\ e_4 = 0\} \tag{17b}$$

$$Surface\,3 \quad S_1^2 := \{\mathbf{e} : e_2 = e_4 = 0\} \tag{17c}$$

where the subscript and superscript denote the dimension and the number of the discontinuity surfaces, respectively. The surface S_1^2 is the intersection of the surfaces S_1^3 and S_2^3. The detailed proof of existence and continuation of the solution is not presented for the sake of brevity. The uniqueness analysis of the Filippov's solution is next carried out for the discontinuity surface, S_1^3. The discontinuity surface S_1^3 divides the solution region into: $\Omega^+ := \{\mathbf{e} : e_2 > 0\}$ and $\Omega^- := \{\mathbf{e} : e_2 < 0\}$. The normal to this surface, $\mathbf{N}_{\mathbf{S_1^3}}$, is:

$$\mathbf{N}_{\mathbf{S_1^3}} = \left\{ \frac{\partial S_1^3}{\partial e_1} \quad \frac{\partial S_1^3}{\partial e_2} \quad \frac{\partial S_1^3}{\partial e_3} \quad \frac{\partial S_1^3}{\partial e_1} \right\} = \{0 \quad 1 \quad 0 \quad 0\}^T \tag{18}$$

Defining the vector functions $\mathbf{f}^+$ and $\mathbf{f}^-$ as the limiting values of the right-hand sides of (10) in Ω^+ and Ω^-, the projections of $\mathbf{f}^+$ and $\mathbf{f}^-$ along the normal to the discontinuity surface, S_1^3, are:

$$\mathbf{f}_{\mathbf{N_1^3}}^+ = \mathbf{f}^+ \cdot \mathbf{N}_{\mathbf{S_1^3}} = \frac{A}{m} e_3 - \frac{F_S}{m} - \frac{\widetilde{F}_{imp}}{m} \tag{19a}$$

$$\mathbf{f}^{-}_{\mathbf{N}_1^3} = \mathbf{f}^{-} \cdot \mathbf{N}_{\mathbf{S}_1^3} = \frac{A}{m} e_3 + \frac{F_S}{m} - \frac{\widetilde{F}_{imp}}{m} \tag{19b}$$

Therefore: $$\mathbf{f}^{+}_{\mathbf{N}_1^3} - \mathbf{f}^{-}_{\mathbf{N}_1^3} = -2\frac{F_S}{m} < 0 \tag{20}$$

Thus, according to Filippov [4], the uniqueness of the Filippov's solution for equations (10) is guaranteed. The uniqueness analysis for S_2^3 can be in a similar way. Uniqueness analysis of S_1^2 requires heavier mathematical machinery and is not detailed.

5 Stability Analysis

In this section, the extension of LaSalle's invariance principle to nonsmooth systems is employed to prove that all the solution trajectories converge to the equilibria. Two positive smooth regular functions are constructed for contact and noncontact phases of motion. Each function guarantees the convergence of the system trajectories to the system's largest invariant set, proven to contain only the points belonging to equilibria. Combination of both functions results in a continuous composite regular function.

Noncontact region: In the noncontact region, the scalar function V_n is defined as:

$$V_n = \frac{K_p C^2}{2m\left(K_p A - K_x C\right)}\left(\frac{A e_1}{C} + e_3\right)^2 + \frac{1}{2}e_2^2 + \frac{C}{2m}e_3^2 + \frac{\tau\, c_d w A}{2mk_{sp}\sqrt{\rho}\left(K_p A - K_x C\right)}e_4^2 \tag{21}$$

which is positive as long as $K_p A - K_x C > 0$. This leads to the condition:

$$\frac{K_p}{K_x} > \frac{C}{A} \tag{22}$$

on the control gains. The derivative of V_n is

$$\dot{V}_n = -\frac{c_d w A}{k_{sp}\sqrt{\rho}\, m\left(K_p A - K_x C\right)}\left(e_4^2 + \frac{k_{sp}K_p e_3^2|e_4|}{\sqrt{P_s - sign(e_4)\, e_3}}\right) - \frac{\left(F_C + (F_S - F_C)e^{-(e_2/\dot{x}_s)^2}\right)}{C}|e_2| - \frac{d}{C}e_2^2 \tag{23}$$

which is continuous and negative semi-definite throughout the noncontact region.

Contact region: In contact region $(e_1 > 0)\,\&\,(1 + pe_2 > 0)$, the positive scalar function is defined as:

$$V_c = \frac{K_p C^2}{2m\left(K_p A - K_x C\right)}\left(\frac{A e_1}{C} + e_3\right)^2 + \frac{1}{2}e_2^2 + \frac{C}{2m}e_3^2 + \frac{\tau\, c_d w A}{2mk_{sp}\sqrt{\rho}\left(K_p A - K_x C\right)}e_4^2 + \frac{H}{(n+1)m}e_1^{n+1} \tag{24}$$

Differentiation of the above regular function yields

$$\dot{V}_c = -\frac{c_d w A}{k_{sp}\sqrt{\rho}\, m\left(K_p A - K_x C\right)}\left(e_4^2 + \frac{k_{sp}K_p e_3^2|e_4|}{\sqrt{P_s - sign(e_4)\, e_3}}\right) - \frac{pH}{m}e_2^2 e_1^n - \frac{\left(F_C + (F_S - F_C)e^{-(e_2/\dot{x}_s)^2}\right)}{C}|e_2| - \frac{d}{C}e_2^2 \tag{25}$$

which is continuous and negative semi-definite in the contact region. The overall composite regular function, V, can now be constructed as:

$$V = \begin{cases} V_n & ; \quad noncontact \\ V_c & ; \quad contact \end{cases} \tag{26}$$

Note that, transition between contact and noncontact regions of motion is dependent on two conditions. When $e_1 > 0$ and $e_2 > (-1/p)$, the system enters the contact region and when $e_1 \le 0$ and/or $e_2 \le (-1/p)$, it transfers to the noncontact region. However, for any positive approach velocity, p is normally a positive small value and *-1/p* is negative and large. Thus, the condition on $(1 + pe_2)$ does not normally contribute to the judgment of noncontact to contact state change and the state change is judged by only the sign of displacement state error, e_1. The only case where the condition $1 + pe_2 > 0$ can be lost while $e_1 > 0$ is when the control force is relatively larger than the impact force and is applied in the opposite direction of the impact force. This rare case is excluded from the stability analysis. Thus, V is a continuous function throughout the solution region.

Derivative of V is derived from combining $\dot{V}_n$ and $\dot{V}_c$ in (23) and (25) that were shown to be continuous and negative semi-definite throughout the solution region except the discontinuity surfaces. On the discontinuity surface, S_1^3:

$$\dot{V}(\mathbf{e} \in S_1^3) \in co[\dot{V}^{S_1^{3+}}, \dot{V}^{S_1^{3-}}] \tag{27}$$

where $\dot{V}^{S_1^{3+}}$ and $\dot{V}^{S_1^{3-}}$ are the limit values of $\dot{V}$ as a solution trajectory approaches S_1^3 from both sides:

$$\dot{V}^{S_1^{3+}} = \lim_{e_4 \to 0^+}\dot{V} = \begin{cases} -\frac{\left(F_C + (F_S - F_C)e^{-(e_2/\dot{x}_s)^2}\right)}{C}|e_2| - \frac{d}{C}e_2^2 & noncontact \\ -\frac{pH}{m}e_2^2 e_1^n - \frac{\left(F_C + (F_S - F_C)e^{-(e_2/\dot{x}_s)^2}\right)}{C}|e_2| - \frac{d}{C}e_2^2 & contact \end{cases}$$

$$\dot{V}^{S_1^{3-}} = \lim_{e_4 \to 0^-}\dot{V} = \begin{cases} -\frac{\left(F_C + (F_S - F_C)e^{-(e_2/\dot{x}_s)^2}\right)}{C}|e_2| - \frac{d}{C}e_2^2 & noncontact \\ -\frac{pH}{m}e_2^2 e_1^n - \frac{\left(F_C + (F_S - F_C)e^{-(e_2/\dot{x}_s)^2}\right)}{C}|e_2| - \frac{d}{C}e_2^2 & contact \end{cases} \tag{28}$$

Equations (28) imply that the convex set described in (27) only contains negative elements. Thus, on the surface S_1^3:

$$\dot{V}(\mathbf{e} \in S_1^3) = \overline{co}\left[-\frac{pH}{m}e_2^2 e_1^n - \frac{\left(F_C + (F_S - F_C)e^{-(e_2/\dot{x}_s)^2}\right)}{C}|e_2| - \frac{d}{C}e_2^2,\; -\frac{\left(F_C + (F_S - F_C)e^{-(e_2/\dot{x}_s)^2}\right)}{C}|e_2| - \frac{d}{C}e_2^2\right] \tag{29}$$

We can now conclude that $\dot{V}$ is negative semi-definite in both regions of contact and noncontact motion as well as on the discontinuity surface, S_1^3. Similar proof can be derived for the derivative of V on S_2^3 and S_1^2 but is not presented for brevity. Therefore, according to the extended LaSalle's invariance principle to nonsmooth systems, every solution trajectory in Ω converges to the largest invariant set, M, as $t \to \infty$. It is next proven that the largest invariant set, M, contains only the equilibria. This is proven by contradiction. Let R be the set of all points within the solution region Ω where $\dot{V} = 0$. According to (23) and (25), $\dot{V} = 0$ requires that for all the points in R, $e_2 = 0$ and $e_4 = 0$. Thus, both $\dot{e}_2$ and $\dot{e}_4$ are zero. Let M be the largest invariant set in R and contain a point where at least one of the error states, e_1 or e_3 is not equal to the values shown in (14). According to equations (10b) and (10d), this will result in $\dot{e}_2 \neq 0$ and/or $\dot{e}_4 \neq 0$ which necessitates the solution trajectory to immediately move out of the set R and certainly set M. But, this conclusion contradicts the initial assumption that M is the largest invariant set in R. Thus, both error states e_1 and e_3 can only be equal to the values shown in (14) and every solution trajectory in Ω converges to the largest invariant set M containing only the system's equilibria.

The above discussion concludes that as long as $K_p/K_x > C/A$, the control system (10) is guaranteed to converge to the system's equilibria. On the other hand, it was earlier shown that in order to decrease the position steady-state error, we have to decrease K_p/K_x. Therefore, in the presence of friction, the smallest possible range of the system's position steady-state error would be when K_p/K_x is equal to C/A.

When the system has negligible friction, the only discontinuity surface of the system is S:={**e**: $e_4 = 0$} and the system has the unique equilibrium point $\mathbf{e}_{eq} = (0,0,0,0)^T$. Stability analysis can, then, be conducted using the positive-definite Lyapunov function defined in (26) with condition (22) on the control gains. The new derivative of the Lyapunov function would be:

$$\dot{V} = \begin{cases} -\dfrac{c_d w A}{k_{sp}\sqrt{\rho}\, m\left(K_p A - K_x C\right)}\left(e_4^2 + \dfrac{k_{sp} K_p e_3^2 |e_4|}{\sqrt{P_s - \mathrm{sgn}(e_4)\, e_3}}\right) & \text{noncontact} \\ -\dfrac{c_d w A}{k_{sp}\sqrt{\rho}\, m\left(K_p A - K_x C\right)}\left(e_4^2 + \dfrac{k_{sp} K_p e_3^2 |e_4|}{\sqrt{P_s - \mathrm{sgn}(e_4)\, e_3}}\right) - \dfrac{pH}{m} e_2^2 e_1^n & \text{contact} \end{cases} \quad (30)$$

which is negative and semi-definite. Similar to the analysis of the system with friction, it can be proven that $\dot{V}$ is also negative on the discontinuity surface, S. Therefore, based on the theorem outlined in [5], the equilibrium point of the system, $\mathbf{e}_{eq} = (0,0,0,0)^T$, is asymptotically stable.

6 Experimental Verification

Experiments were conducted on an electrohydraulic actuator test rig and metal and wooden blocks were used to represent different environmental stiffnesses.

6.1 Test Rig

The hydraulic circuit consists of an actuator controlled by a Moog D765 servovalve, mounted on a reinforced steel table. The servovalve can flow 34 *L/min* at 3000 *psi* and has a rise time of 2 *ms*. It uses a mechanical feedback spring with a linear variable differential transformer (LVDT) that measures the position of the spool. A rotary encoder with a resolution of 1024 *counts/revolution* (linear resolution of 0.0011 *in*) establishes the relative position of the actuator. An S-beam type load cell detects the first nonzero contact force between the actuator and the environment. The hard and soft environments are resembled by metal and wooden blocks bolted to an I-beam mounted to the test station base.

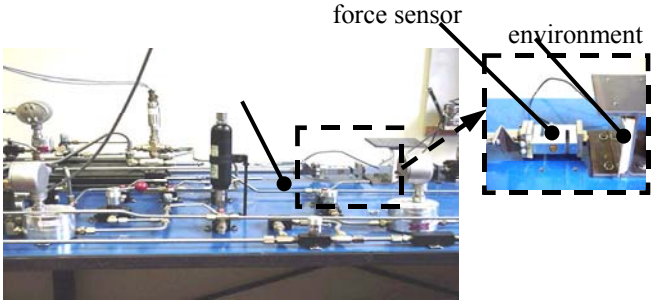

Fig. 2 Schematic of the experimental test rig.

6.2 Experimental Results

In all experiments, the actuator accelerated from free space given a step input control signal and struck the environment. Upon sensing a nonzero force for the first time, control was switched to the proposed control law (12) until the actuator was stabilized on the surface of the environment. The position corresponding to the first nonzero force was taken as the position of the environment surface. Similar supply pressures, P_s =1900 *psi* was used in each set of experiment and the sampling time of the system was approximately 2 *ms*. The approximate hydraulic compliance of the test rig was estimated as C=7.14x10^{-5} in^3/psi. Knowing A=0.98 in^2, the control gains were chosen as K_x=1.3 $V/in\sqrt{psi}$ and K_p=1.4×10^{-5} $V/\sqrt{psi^3}$ which satisfied (22). Given the approximate value of F_S, which was experimentally determined as 314.72 *lbf*, the steady-state position and pressure differential errors were calculated to be in the range of $e_{1ss} \in [-3.5\text{x}10^{-3}, 1.45\text{x}10^{-3}]\,in$ and $e_{3ss} \in [-135, 325]\,psi$ for the aluminum block, and $e_{1ss} \in [-3.5\text{x}10^{-3}, 2.4\text{x}10^{-3}]\,in$ and $e_{3ss} \in [-223, 325]\,psi$ for

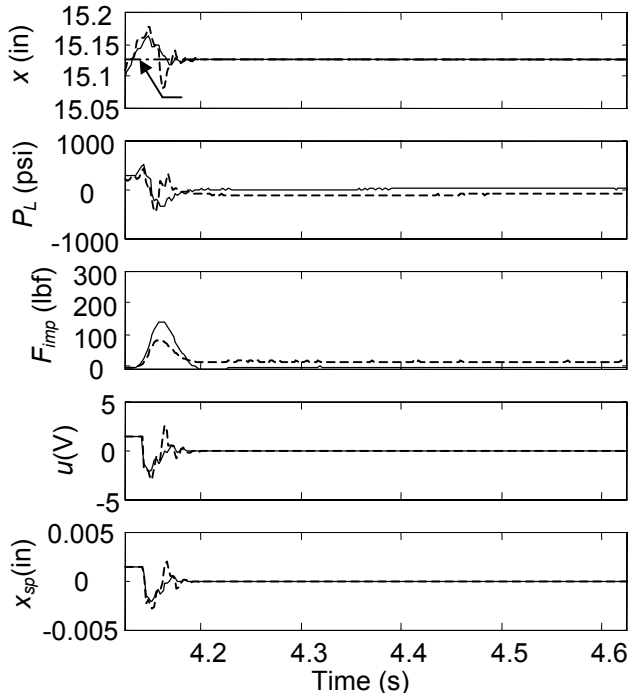

Fig. 3 Low velocity response (3 *in/s*); wooden block ---, metal block ——.

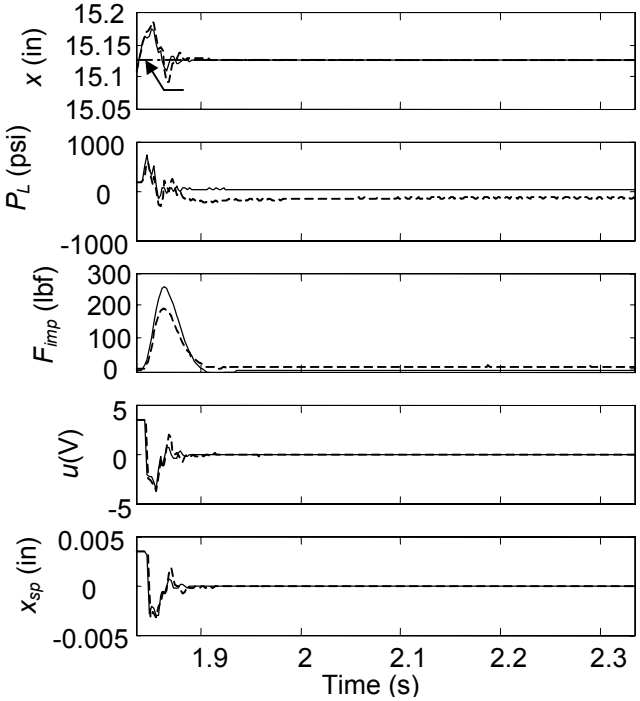

Fig. 4 High velocity response (8 *in/s*); wooden block --- , metal block ——.

the wood block [see (14) and (16) for calculation of the bounds]. Note that for aluminum block H=3.32×10^6 *lbf/in*$^{1.5}$, and for the wood block H=0.84×10^6 *lbf/in*$^{1.5}$.

Figures 3 and 4 show the responses when the actuator hits the above two types of environments with low (3 *in/s*) or high (8 *in/s*) approach velocities. They clearly verify that the proposed controller is capable of stabilizing the actuator around the surface of the environment regardless of the environment stiffness and the magnitude of the approach velocity. It is also seen that the final state of the system in all trials is, indeed, where $x_{sp} = 0$, $\dot{x} = 0$, and x is in a close vicinity of the surface of the environment.

7 Conclusions

A Lyapunov-based discontinuous controller was developed for hydraulic actuators to regulate the impacts during transition phase from free-space to constraint motion. The scheme does not require force or velocity feedback as they are difficult to measure throughout the short transition phase. Stability and effectiveness of the control scheme considering realistic Hertz-type impact model, practical friction model, hydraulic nonlinearities, and servovalve dynamics were verified both analytically and experimentally. The extension of LaSalle's invariance principle to nonsmooth systems was employed to prove that all the solution trajectories converge to the equilibria with position steady state errors bounded in a small range adjustable by selecting proper controller gains based on Lyapunov stability analysis. Experiments confirmed that the proposed controller could stabilize the actuator during the transition from free to constrained motion.

References

[1] Pagilla, P. R., and Yu, B., "A stable transition controller for constrained robots", *IEEE/ASME Transactions on Mechatronics* 6(1): 65-74, 2001.

[2] Xu, W. L., Han, J. D., and Tso, S. K. "Experimental study of contact transition control incorporating joint acceleration feedback", *IEEE/ASME Transactions on Mechatronics* 5(3): 292-301, 2000.

[3] Tarn, T. J., Wu, Y., Xi, N., and Isidori, A., "Force regulation and contact transition control", *IEEE Control Systems* 16(1): 32-40, 1996.

[4] Filippov, A. F., Differential equations with discontinuous right-hand sides. Kluwer Academic Publishers, 1988.

[5] Wu, Q., Onyshko, S., Sepehri, N. and Thornton-Trump, A.B., "On Construction of smooth Lyapunov functions for non-smooth systems", *International Journal of Control*, 69: 443-457, 1998.

[6] Merritt, H. E., *Hydraulic Control Systems*, John Wiley, NY, 1967.

[7] Liu, R., and Alleyne, A., "Nonlinear Force/Pressure Tracking of an Electro-Hydraulic Actuator", *ASME J. Dyn. Syst, Meas., and Cont.* 122: 232-237, 2000.

[8] Gilardi, G., and Sharf, I., "Literature survey of contact dynamics modeling", *Mech. Mach. Theory*, 37: 1213-1239, 2002.

[9] Tafazoli, S., de Silva, C. W., and Lawrence, P. D., "Tracking control of an electrohydraulic manipulator in the presence of friction", *IEEE Transactions on Control Systems Technology*, 6(3): 401-411, 1998.